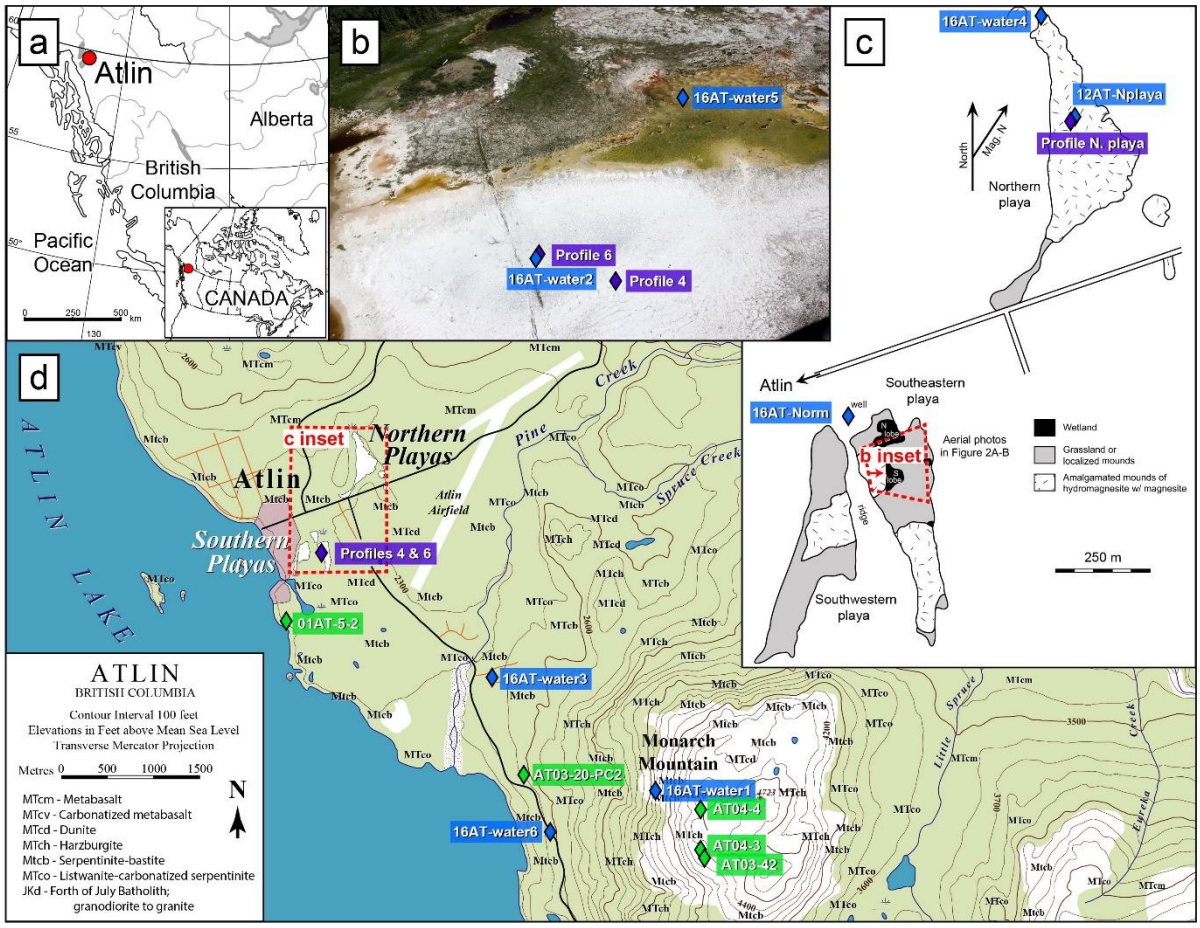

Figure 1. (a) Location of Atlin, British Columbia, Canada. (b) Aerial photograph of the southeastern playa showing the sampling locations for profiles 4 and 6. (c) Map illustrating the northern, southwestern, and southeastern playas near Atlin. (d) Topographic map of the Atlin region (after Energy, Mines, and Resources Canada) including geologic mapping by Ash and Arksey (1990). Sample locations for ultramafic bedrock samples (green), sediments (purple), and waters (blue) collected for this study are given (samples listed in Table 1).

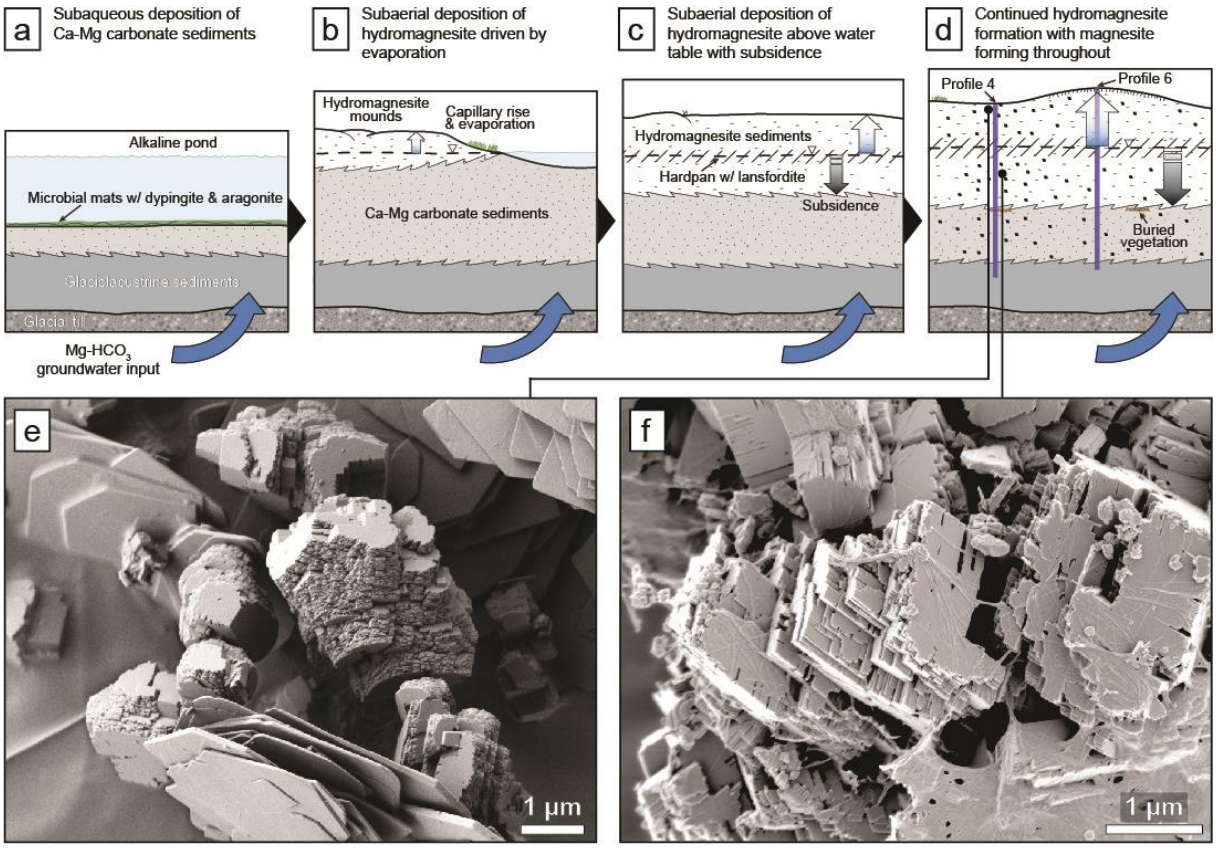

Figure 2. Conceptual diagrams of a simplified model for the subaqueous deposition of Ca-Mg carbonate sediments (a) followed by subaerial deposition of hydromagnesite mounds (b and c) driven by evaporation and latter formation of magnesite (d). (e) Representive scanning electron micrograph of hydromagnesite (plates) and magnesite (exhibiting spiral crystal growth) from above the water table in profile 4. (f) Representative micrograph of magnesite with a blocky crystal morphology from below the water table in profile 4.

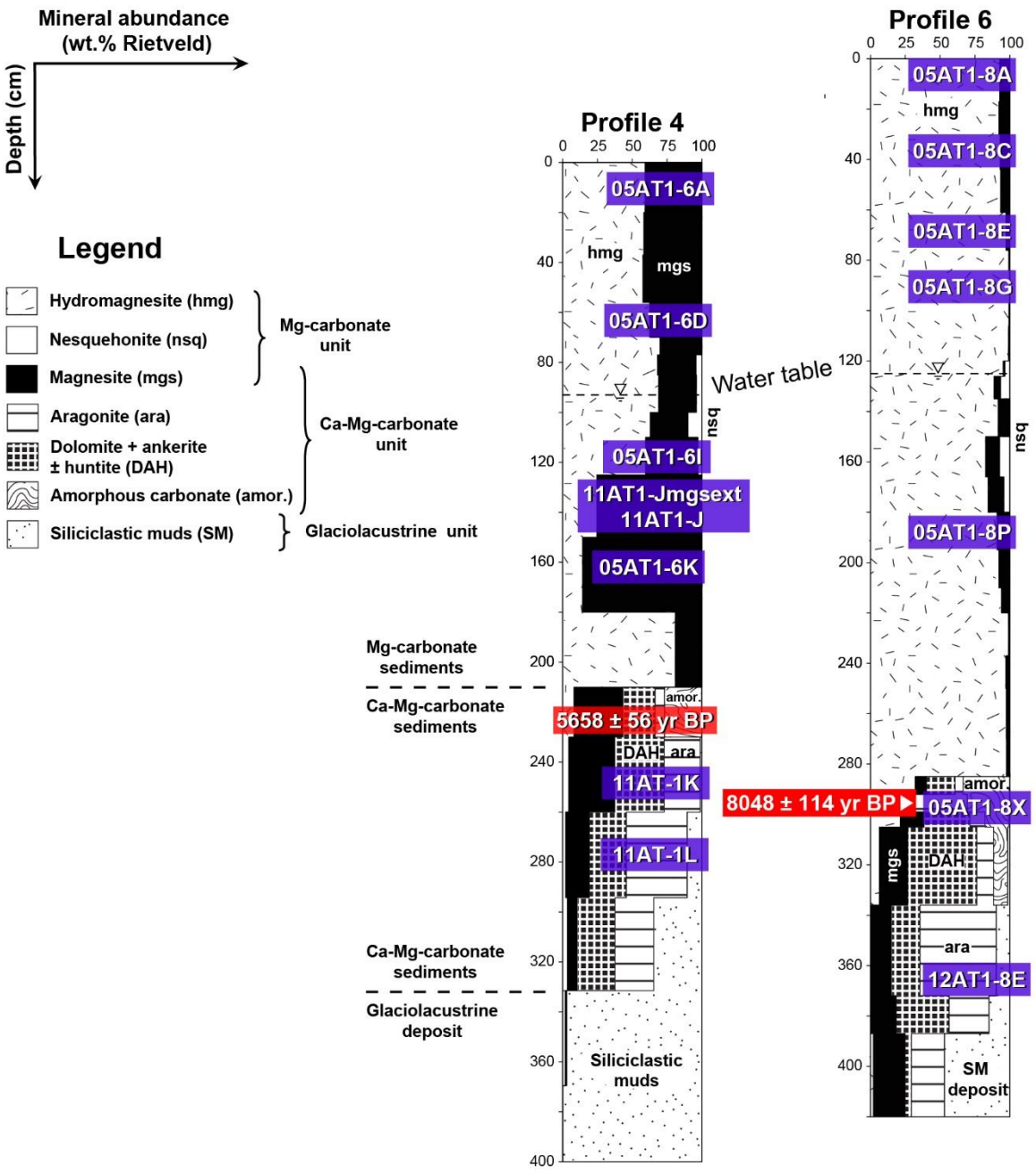

Figure 3. Mineral abundance profiles 4 and 6 from Power et al. (2019). Mineral abundances (wt.%) *versus* depth (cm). The minerals plotted include hydromagnesite (hmg), magnesite (mgs), nesquehonite (nsq), aragonite (ara), dolomite, ankerite and huntite (grouped as DAH), and silicate minerals grouped as siliciclastic muds. The calibrated ages are based on radiocarbon analyses of organic material. The sediment profiles are positioned vertically based on their relative elevations.

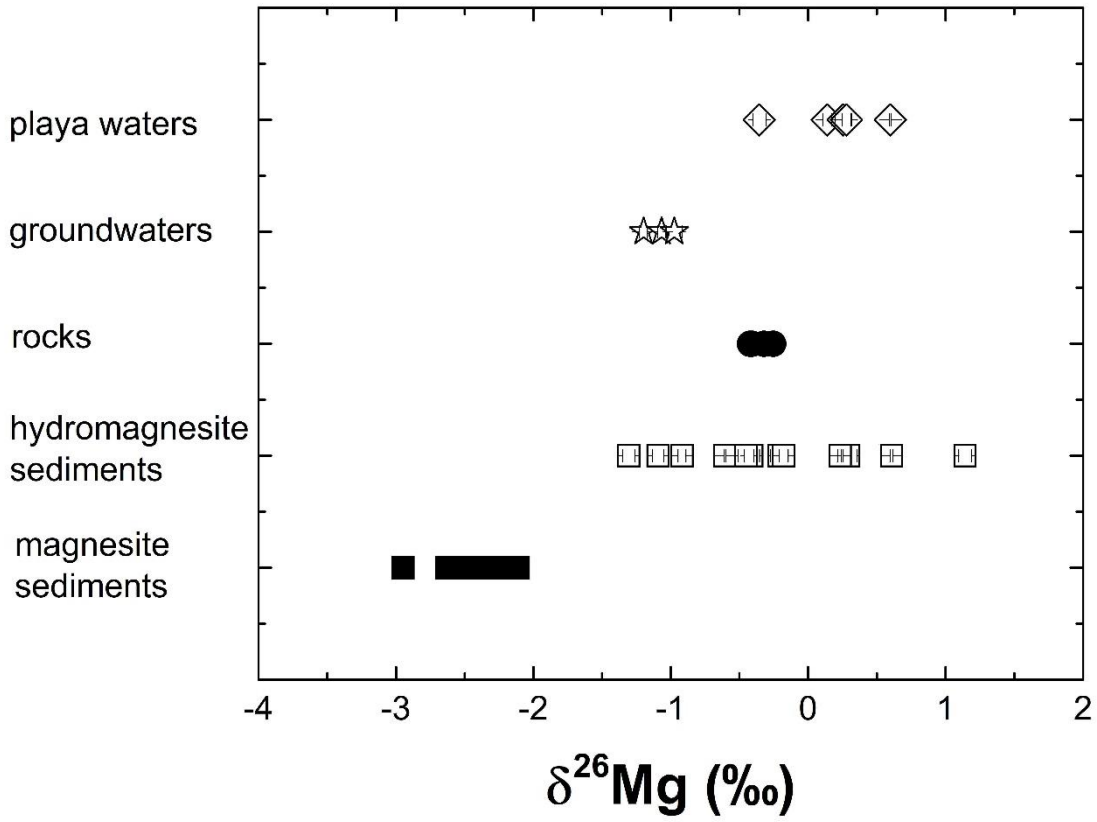

Figure 4: Magnesium isotope composition of waters and solid reservoirs analyzed in this study. "Magnesite sediments" are defined as solids with more than 85 wt % magnesite and/or solids containing other anhydrous carbonate minerals such as dolomite, calcite, aragonite and huntite. "Hydromagnesite sediments" are defined as those containing more than 60 wt.% hydromagnesite. For detailed mineralogic composition refer to Table 1.

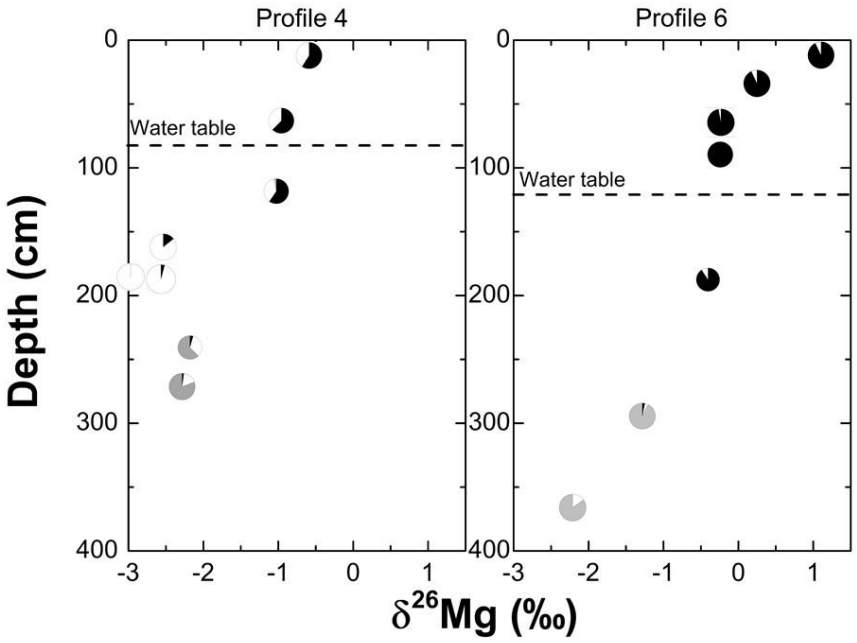

Figure 5: Magnesium isotope composition of sediment samples in profiles 4 and 6 as a function of depth. The black area in the pie charts denotes the wt.% of hydromagnesite and the white that of magnesite. The grey colour represents the wt. % of other phases (for details see Table 1). Analytical errors are included in the symbol size.

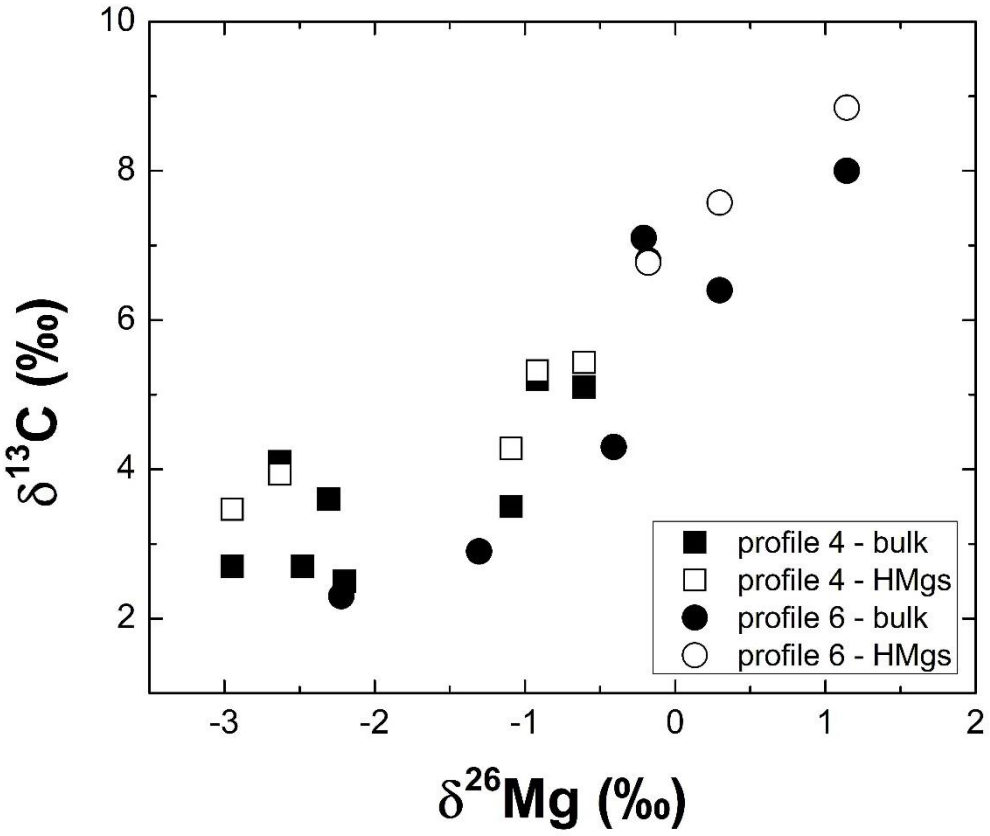

Figure 6: Carbon *vs.* Magnesium isotope composition of sediments from profiles 4 and 6. To covariation of the isotope compositions of the sediments yield a R^2=0.71 and $p<0.05$. Bulk $\delta^{13}C$ compositions of samples are reported in Power et al. (2014), whereas the $\delta^{13}C$ composition of hydromagnesite can be found in Power et al (2019). Analytical errors are included in the symbol size.

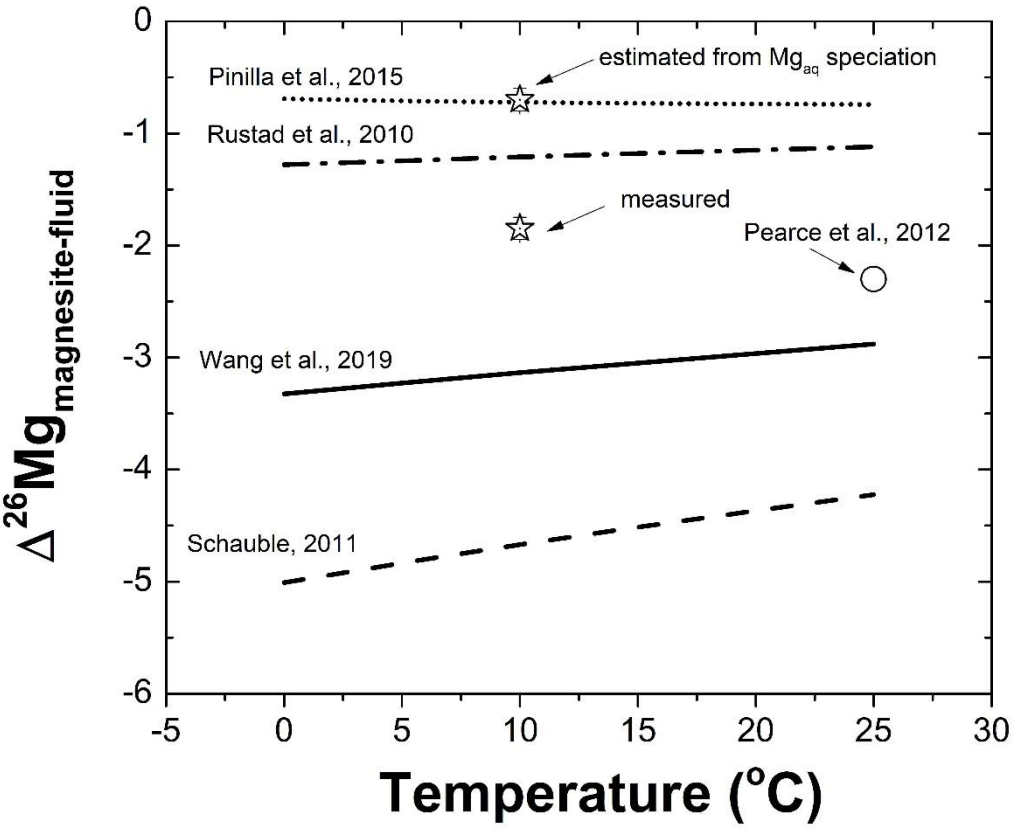

Figure 7: Magnesium isotope fractionation between magnesite and fluid as a function of temperature defined in theoretical studies compared to the results of this study. The isotopic fractionation of measured samples has been estimated assuming a fluid composition of -1.1‰.